Theor Chem Acc (2000) 104:257–264
DOI 10.1007/s002140000158

Theoretical
Chemistry Accounts

Regular article

Azido-, hydroxo-, and oxo-bridged copper(II) dimers: spin population analysis within broken-symmetry, density functional methods

Catherine Blanchet-Boiteux, Jean-Marie Mouesca

Laboratoire de Métalloprotéines, Magnétisme et Modèles Chimiques, Service de Chimie Inorganique et Biologique, UMR 5046, Département de Recherche Fondamentale sur la Matière Condensée, CEA-Grenoble, 17 rue des Martyrs, 38054 Grenoble Cedex 9, France

Received: 17 September 1999 / Accepted: 9 March 2000 / Published online: 21 June 2000

Abstract. Within the general context of homometallic spin-coupled Cu(II) dimers, we propose to relate the antiferromagnetic part of the exchange coupling constant, J_{AF}, to the quantity $\Delta P^2(\mathrm{Cu})$, the difference of copper squared spin populations as calculated for the high-spin (i.e. triplet) and broken-symmetry spin states, through $J_{AF} \approx -U\Delta P^2(\mathrm{Cu})$, where U is interpreted as the covalent–ionic term. This proportionality is illustrated for three "bare" Cu(II) dimers (i.e. without peripheral ligation, so as to enhance the antiferromagnetic contribution) bridged by azido, hydroxo, or oxo groups. This provides an alternative quantifier of the exchange phenomenon to that usually used, i.e. Δ^2, the square of the singly occupied molecular orbital splitting in the triplet state. Moreover, and quite interestingly, the quantity $\Delta P^2(\mathrm{Cu})$ can become negative (i.e. induce ferromagnetism) without apparently affecting the proportionality relation.

Key words: Exchange coupling – Antiferromagnetism – Valence-bond – Broken-symmetry – Spin populations

1 Introduction

In the search for efficient ferromagnetic couplers, the end-on azido [1–6] and the hydroxo [7, 8] units count among the best ones currently available, whereas the oxo bridge has been presented recently as such on computational grounds [9] (although still without firm theoretical justification).

Models [10–15] have been developed in the last 30 years to understand the magnetic properties of binuclear metal complexes, in general, and copper dimers, in particular. The singlet–triplet energy gap is then expressed as the sum of ferromagnetic, J_F, and antiferromagnetic, J_{AF}, contributions, the latter usually being dominant as the magnetic orbital overlap increases (this is presented in more detail in Sect. 2). Orthogonality, or accidental degeneracy, of the two magnetic orbitals would therefore be the common way to get ferromagnetism, for example, by varying the Cu-bridge-Cu bridging angle. The crossover of the magnetic orbitals would thus occur around 108° for the end-on azide species [16, 17], against 98° for μ_2-hydroxo species [7], for example.

More generally, it is therefore crucial to be able to identify and understand the main ferromagnetic mechanisms in these complexes (accidental degeneracy of the magnetic orbitals, spin polarization, etc., see later) and to be able to quantify properly both ferromagnetic and antiferromagnetic contributions (for the latter ones, this is usually done within the context of the molecular orbital (MO) formalism, see Sect. 2).

The point of this contribution is not to discuss the intricacies rationalizing the observed (or computed) ferromagnetism exhibited by these species, especially by the azido-bridged species [4, 5, 15]: this issue has been addressed elsewhere by the same authors [18, 19]. Rather, and from a computational point of view, we attempt to calculate the J coupling constants for the three title compounds, as already done by others by density functional theory [6, 9, 20–22] or ab initio techniques [23, 24], stressing how copper spin populations can be used as quantifiers of the (antiferromagnetic part of the) exchange phenomenon (via magneto-structural correlations). In that sense, our spin-population-based contribution will be presented as "computational" evidence (rather than theoretical justification) in favor of our proposal, which exhibits a new twist related to the previously-mentioned race toward better ferromagnetic couplers.

2 Exchange coupling models

At the heart of the valence bond (VB) and MO approaches is the concept of magnetic orbitals, comprising metallic and bridge orbitals mediating the exchange interaction between the two magnetic monomers having unpaired spins. They also implicitly rest on the "active electron approximation", i.e. on the assump-

Correspondence to: J.-M. Mouesca

tion that the bridge orbitals lie much lower in energy than the metallic (and magnetic) *d* orbitals. If this condition is generally verified for electronegative halogeno or oxo/hydroxo bridges, this is not the case for the azido ion, as soon recognized [15]. Equivalently, only the two unpaired electrons (i.e. for copper dimers) are explicitly taken into account in the exchange interaction phenomenon (i.e. the role of the doubly occupied MOs is usually neglected). We briefly present and then quantitatively test three alternative molecular magnetism models, as they appeared in the literature in the 1970s and early 1980s (Sects. 2.1–2.3). We will thus consider a symmetric A-X-B dimer made of metallic ions, surrounded by bridging and terminal ligands and containing only one unpaired electron each as is the case of a Cu(II) dimer.

2.1 MO model

In this approach, the magnetic orbitals (in the absence of interaction) can be derived from the two singly occupied MOs (SOMO), $\Psi_{1,2}$, of the low-lying triplet state. One thus constructs $\Phi'_{A,B} = (1/2^{1/2})(\Psi_1 \pm \Psi_2)$, orthogonal MOs (OMO) which are orthogonal but not strictly localized. Hay et al. [11] derived the following approximate expressions

$$\begin{aligned} J_{AF}^{OMO} &\approx -\frac{\Delta^2}{U} \\ J_{F}^{OMO} &= 2j' \ , \end{aligned} \tag{1}$$

where U is the charge-transfer energy (difference between the covalent A-B and the ionic A^-- B^+ /A^+- B^- configurations), both quantities Δ and $U(\Delta \ll U)$ leading to the "kinetic" (antiferromagnetic) part of the exchange. The ferromagnetic term, j', is the two-electron exchange integral on the basis of Φ'_A and Φ'_B (the "potential" part of the exchange). In the following, in order to distinguish the U values deduced from magneto-structural correlations based on the MO or VB approaches, we write $J_{AF}^{OMO} \approx -\Delta^2/K$ and consider K as a fitting parameter (more on this point in Sect. 3.4).

2.2 VB model

An alternative interpretation of these phenomena goes back to Heitler and London the view of the chemical bond as they expressed the exchange term using localized (VB) orbitals. Following them, Kahn and Briat [25, 26] derived the magnetic orbitals as the highest occupied MOs (HOMO) for the localized A-X and X-B non-orthogonal fragments Φ_A and Φ_B ($S_{AB} = \langle \Phi_A | \Phi_B \rangle$), therefore called natural MOs (NMO). They obtained the following expressions:

$$\begin{aligned} J_{AF}^{NMO} &= -2\frac{\Delta S_{AB}}{1 + S_{AB}^2} \\ J_{F}^{NMO} &= 2(j - kS_{AB}^2) \end{aligned} \tag{2}$$

Δ is, again, the energy gap between the two molecular orbitals in $A - X - B$, now built from the interacting Φ_A and Φ_B in the triplet state. The ferromagnetic j contribution is described as the self-repulsion of the overlap density $\rho_{AB} = \Phi_A \Phi_B$ and k is a Coulombic integral related to $\rho_{AA} = \Phi_A^2$. For $S_{AB}^2 \ll 1$, one utilizes the following approximate expressions: $J_F^{NMO} \approx 2j$ and $J_{AF}^{NMO} \approx -2\Delta S_{AB}$.

2.3 VB–broken-symmetry model

Finally, a (spatially) broken-symmetry (BS) state, $\Psi_{BS}(r_1, r_2)$ can be constructed [27, 28] as an "outer product" of monomer spin functions (i.e. of the two NMOs) as $\Phi_A(r_1)\Phi_B(r_2)$. Ψ_{BS} is thus not an eigenstate of spin but a (artificial) state of mixed spin, which turns out to be computationally very useful. In effect, and from its use, Noodleman [29] derived the following expression for $J_{AF}(S_{AB}^2 \ll 1)$

$$\begin{aligned} J_{AF}^{VB-BS} &\approx -US_{AB}^2 \\ J_{F}^{VB-BS} &= 2j' \ , \end{aligned} \tag{3}$$

which was verified quantitatively [30, 31] and where U is, again, the charge-transfer energy.

2.4 Definition of the quantity $\Delta P^2(Cu)$

Both (MO and VB) approaches [13] stand as two rigorously alternative and equivalent ways of describing the exchange interactions if one properly takes into account covalent–ionic mixing, whereas Noodleman's approach allows the unification of both nonorthogonal VB and (limited) configuration interaction viewpoints [29] in the weak overlap regime, though. Notice also that, as Δ is usually proportional to $S_{AB}, J_{AF} \sim \Delta^2 \sim \Delta S_{AB} \sim S_{AB}^2$.

Both NMOs and OMOs can be related in the following general manner:

$$\begin{aligned} \Phi_A &= \lambda \Phi'_A + \mu \Phi'_B \\ \Phi_B &= \mu \Phi'_A + \lambda \Phi'_B \ , \end{aligned} \tag{4}$$

with $S_{AB} = 2\lambda\mu$ and $\lambda^2 + \mu^2 = 1$. To second order in S_{AB}, $\lambda \approx 1 - S_{AB}^2/8$ and $\mu \approx S_{AB}/2$. As the VB–BS method makes use of these NMOs, [29] one easily derives:

$$\begin{aligned} P_{HS}(\Phi'_A) &= \lambda^2 + \mu^2 \\ P_{BS}(\Phi'_A) &= \lambda^2 - \mu^2 \end{aligned} \Rightarrow \begin{aligned} \lambda^2 &= \frac{P_{HS}(\Phi'_A) + P_{BS}(\Phi'_A)}{2} \\ \mu^2 &= \frac{P_{HS}(\Phi'_A) - P_{BS}(\Phi'_A)}{2} \ , \end{aligned} \tag{5}$$

i.e.

$$S_{AB}^2 = 4\lambda^2\mu^2 = P_{HS}(\Phi'_A)^2 - P_{BS}(\Phi'_A)^2 \ . \tag{6}$$

Equation (6) is actually equivalent to Malrieu's Eq. (14) with $P^{HS} = 1$ where the OMOs are taken to be the copper $d_{A/B}$ atomic orbitals [32].

In practice, one does not calculate the Mulliken spin population of delocalized MOs, but atomic spin populations (here copper ones). As such, this restriction implies that $\Delta P^2(d_{xz})$ becomes strictly equal to S_{AB}^2 only for a negligible weight of the bridging and ligand orbitals

in the magnetic orbitals. It is precisely this transition from $\Phi'_{A,B}$ to $Cu_{A,B}$ which leads from Noodleman's VB expression ($J_{AF} \approx -US^2_{AB}$) to that of Kahn and Briat ($J_{AF} \approx -2\Delta S_{AB}$) through explicitly taking into account the bridging orbitals [19]. In other words, $P_{HS}(\Phi'_A) = \lambda^2 + \mu^2 = 1$ (always true for the partially delocalized OMO Φ'_A, but this is formal), whereas $P_{HS}(Cu_A) < 1$.

We therefore defined the quantity (used extensively in the following sections)

$$\Delta P^2(\mathrm{Cu}) \equiv P_{HS}(\mathrm{Cu_A})^2 - P_{BS}(\mathrm{Cu_A})^2 \ , \qquad (7)$$

which would turn out to be S^2_{AB} in the previous simple treatment for almost purely metallic magnetic orbitals. Notice that Ruiz et al. [33] also proposed quite recently to approximate S^2_{AB} by $P_{HS}(Cu_A)^2 - P_{HS}(Cu_A)^2$ without, however, correlating J to ΔP^2(Cu) as suggested from a comparison of Eqs. (3) and (7). In effect, one can now expect a good correlation to occur between the calculated J_{AF} spin-coupling constant and ΔP^2(Cu), strictly so for small overlap S_{AB} and $J_F \ll |J_{AF}|$. This is verified numerically in Sect. 3.2 and offers an alternative simple way of quantifying J_{AF} to that of Hay et al., though at the price of converging two states (triplet and Ψ_{BS}) instead of only one (the triplet).

3 Calculations on $[Cu_2(bridge)_2]^{2+}$

3.1 Computational details

We performed a series of calculations, all in C_{2v} symmetry, for three Cu(II) complexes with three different bridges (bdg), azido (bdg = N_3^-), hydroxo (OH^-), and oxo (O^{2-}), varying the core geometries through the angle Cu-bdg-Cu (between 80° and 110°). The following axis system was chosen: the z-axis is set along the metal–metal direction, the x-axis along the bdg–bdg direction, and the y-axis perpendicular to the $Cu_2(bdg)_2$ plane. Cores were chosen for two reasons:

1. The complete complexes (i.e. with peripheral ligation) exhibit ferromagnetism, whereas one is interested here in antiferromagnetism. Indeed, external ligands further remove the degeneracy of the 3*d* metal orbitals, leaving the d_{xz} (in our axis system) Cu(II) orbitals at higher energy. This is realized through their interaction with the bridging orbitals (lying in the xz plane) and is actually observed in our computed electronic structures in the B_1 symmetry (C_{2v} calculations) containing these magnetic orbitals. As far as the other four d orbitals are concerned (distributed among the A_1, A_2, and B_2 symmetries), they remain close to degenerate (within 0.2 eV) in the absence of external ligation, but are occupied for both spins (as would be the case in the presence of external ligation in the xz plane) for Cu(II) ions.
2. As $\Delta P^2(\mathrm{Cu}) \sim S^2_{AB}$ quantifies J_{AF}, larger overlaps appear for core dimers, in contrast to ligated ones. While it is true that the systems studied here have no chemical meaning, this does not remove any interest in a theoretical treatment. By adding terminal ligation to the copper(II) ions, the d orbitals (now antibonding metal–ligand orbitals) rise in energy above the bridging orbitals and all the systems tend toward (or actually reach) ferromagnetism. As we are interested here in the antiferromagnetic contribution [to which ΔP^2(Cu) is linked], we artificially removed the terminal ligation so as to increase the effect. Indeed, computational chemistry allows us some freedom in the choice of the systems which "real life" chemistry would abhor (more on this point in Sect. 4).

We chose, therefore, our three model complexes as follows: $[Cu_2(N_3)_2]^{2+}$, $[Cu_2(OH)_2]^{2+}$, and $[Cu_2(O^{2-})_2]^0$, from less to more electronegative bridges. The relevant geometrical features were derived by idealization (symmetrization) of the published structures.

All our calculations make use of the Amsterdam linear combination of atomic orbitals density functional programs (ADF 2.3) developed by Baerends and coworkers [34–38] and Ziegler [39]. We considered only the potential referred to as "VBP" (Vosko, Wilk, and Nusair's exchange and correlation energy [40, 41] completed by nonlocal gradient corrections to the exchange by Becke [42] as well as to the correlation by Perdew [43]).

The copper basis set used here, unless otherwise stated, has been slightly spatially contracted (by using Zn d exponents, hence the notation Cu—Zn), as compared to the standard (Cu—Sd) triple-ζ proposed in the ADF 2.3 package. As illustrated in Table 1 for the azido-bridged Cu(II) dimer, this dramatically improves both spin populations (the NMOs relocalize in BS) and energetics (comparing E_{HS}s and E_{BS}s). Upon applying this spatial contraction, the overlap S_{AB} is reduced and the systems are less antiferromagnetic. If this substitution is not that dramatic without terminal ligation, this is another story when "real" complexes are studied. In another article [18], we showed that in some cases there might be a deficiency in the standard copper basis sets commonly used. We did not aim, however, at constructing exact and new copper basis sets, only at mentioning the effect.

We calculate J using the conventional Heisenberg spin Hamiltonian $H = -JS_AS_B$ (hence $J > 0$ for ferro-

Table 1. High-spin/broken-symmetry copper spin populations, quantity ΔP^2(Cu), high-spin/broken-symmetry state energies (eV), computed J_{DFT} values (cm^{-1}, from Eq. 8), (*SOMO*) gap Δ (eV: majority spin) and corresponding two (*LUMO*) gap Δ^* (eV: minority spin) for the azido-bridged Cu(II) "core" dimer. These results are given as obtained for two copper basis sets, a standard one (Cu—Sd) provided by ADF and a (spatially) more contracted one of our own making (Cu—Zn: see main text)

Bare cation	Cu—Sd	Cu—Zn
P_{HS}(Cu)	0.479	0.560
P_{BS}(Cu)	0.065	0.416
ΔP^2(Cu)	0.225	0.141
E_{HS} (eV)	−24.920	−26.488
E_{BS} (eV)	−25.448	−26.799
J_{DFT} (cm^{-1})	−8518	−5033
Δ	1.624	1.507
Δ^*	1.343	1.029

magnetic coupling). We then define the quantity J_S ($= J_F + J_{AF}$), expressed as [28, 29]

$$J_S = \frac{2(E_{BS} - E_T)}{1 + S_{AB}^2} \equiv \frac{J_{DFT}}{1 + S_{AB}^2} \quad . \tag{8}$$

The subscript "S" indicates that the overlap S_{AB} appears explicitly in Eq. (8), and J_{DFT} is defined as J_S ($S_{AB} = 0$). Our computational results are reported in Tables 1–5.

3.2 J_{DFT} as a function of $\Delta P^2(Cu)$

Plots of J_{DFT} as a function of ΔP^2(Cu) for the three dimers are shown in Fig. 1. These plots are rather linear as expected, converging around $J \approx 0$ for $\Delta P^2(Cu) \approx 0$ on the scale used (there is actually a remanent ferromagnetism, cf. Tables 2–4). The least linear plot is obtained for the oxo dimer. A rough estimation of the slope yields $U_{azido} \approx 4.5\,eV$, $U_{hydroxo} \approx 2.5\,eV$, and $U_{oxo} \approx 5.5\,eV$ (from the 80–95° θ range). These values are to be compared with 6.5 eV obtained from photoelectron spectroscopy of copper chlorides [44] and with 5.9 eV (Anderson's estimate [10]).

3.3 J_{DFT} as a function of $-2\Delta S_{AB}$

We compare J_{DFT} to $-2\Delta S_{AB}$ in Fig. 2, thus putting to the test Kahn's VB model. Such a comparison is the

Table 2. High-spin/broken-symmetry copper spin populations, quantity ΔP^2(Cu), high-spin/broken symmetry state energies (eV), computed J_{DFT} values (cm^{-1}, from Eq. 8), SOMO gap Δ (eV: majority spin) and corresponding two LUMO gap Δ^* (eV: minority spin) for the azido-bridged Cu(II) "core" dimer as a function of the Cu—N—Cu angle Θ. These results are given as obtained for the Cu—Zn copper basis set (see main text)

Θ	80°	85°	90°	95°	100°	105°	110°
P_{HS}(Cu)	0.537	0.548	0.553	0.553	0.547	0.537	0.520
P_{BS}(Cu)	0.447	0.447	0.431	0.394	0.344	0.274	0.184
ΔP^2(Cu)	0.088	0.101	0.121	0.150	0.181	0.213	0.236
E_{HS} (eV)	−25.980	−26.251	−26.417	−26.466	−26.414	−26.227	−25.899
E_{BS} (eV)	−26.091	−26.385	−26.592	−26.699	−26.715	−26.601	−26.338
J_{DFT} (cm^{-1})	−1799	−2157	−2813	−3759	−4847	−6025	−7075
Δ	1.101	1.144	1.208	1.288	1.359	1.414	1.426
Δ^*	0.749	0.778	0.834	0.921	1.008	1.087	1.135

Table 3. High-spin/broken-symmetry copper spin populations, quantity ΔP^2(Cu), high-spin/broken-symmetry state energies (eV), computed J_{DFT} values (cm^{-1}, from Eq. 8), SOMO gap Δ (eV: majority spin) and corresponding two LUMO gap Δ^* (eV: minority spin) for the hydroxo-bridged Cu(II) "core" dimer as a function of the Cu—O—Cu angle Θ. These results are given as obtained for the Cu—Zn copper basis set (see main text)

Θ	80°	85°	90°	95°	100°	105°	110°
P_{HS}(Cu)	0.672	0.678	0.680	0.677	0.671	0.661	0.646
P_{BS}(Cu)	0.685	0.679	0.661	0.627	0.576	0.510	0.424
ΔP^2(Cu)	−0.017	−0.002	0.024	0.064	0.118	0.177	0.237
E_{HS} (eV)	−0.953	−1.377	−1.672	−1.842	−1.899	−1.819	−1.591
E_{BS} (eV)	−0.910	−1.350	−1.674	−1.890	−2.010	−2.005	−1.858
J_{DFT} (cm^{-1})	+701	+443	−32	−766	−1743	−2999	−4299
Δ	0.360	0.457	0.583	0.727	0.816	1.001	1.095
Δ^*	0.107	0.203	0.333	0.488	0.653	0.803	0.932

Table 4. High-spin/broken-symmetry copper spin populations, quantity ΔP^2(Cu), high-spin/broken-symmetry state energies (eV), computed J_{DFT} values (cm^{-1}, from Eq. 8), SOMO gap Δ (eV: majority spin) and corresponding two LUMO gap Δ^* (eV: minority spin) for the oxo-bridged Cu(II) "core" dimer as a function of the Cu—O—Cu angle Θ. These results are given as obtained for the Cu—Zn copper basis set (see main text)

Θ	80°	85°	90°	95°	100°	105°	110°
P_{HS}(Cu)	0.402	0.389	0.370	0.338	0.305	0.275	0.239
P_{BS}(Cu)	0.166	0.245	0.288	0.305	0.295	0.273	0.231
ΔP^2(Cu)	0.133	0.092	0.054	0.021	0.006	0.001	0.004
E_{HS} (eV)	−13.821	−13.844	−13.779	−13.611	−13.395	−13.178	−12.857
E_{BS} (eV)	−14.247	−14.170	−14.006	−13.730	−13.441	−13.179	−12.837
J_{DFT} (cm^{-1})	−6866	−5258	−3662	−1928	−732	−18	+332
Δ	1.036	0.920	0.792	0.633	0.515	0.446	0.431
Δ^*	1.239	1.160	1.088	1.034	1.037	1.093	1.252

most natural, as one considers both Eqs. (2) and (8). We again used both Δ and Δ^* and estimated S_{AB} from $S_{AB} \approx \Delta P^2(\mathrm{Cu})^{1/2}$ [with, however, $S_{AB} = 0$ when $\Delta P^2(\mathrm{Cu}) < 0$]. The more electronegative the bridge, the better the agreement between J_{DFT} and $-2\Delta S_{AB}$ (see diamonds in Fig. 2) as the VB expression was derived within the "active electron" approximation. For the azido and the hydroxo bridges, again, the use of Δ^* gaps yields better results.

3.4 J_{DFT} as a function of Δ^2/Δ^{*2}

We then tested the model of Hay et al. by plotting J_{DFT} as a function of either Δ^2 (splitting of the SOMOs, say of α spin) or Δ^{*2} (the corresponding empty orbitals of β spin). The use of Δ^* as an alternative to that of Δ has already been proposed [45], as metal–ligand orbital mixing sometimes splits the higher majority spin MOs, leaving meaningless SOMOs as a result. This mixing/splitting does not occur as dramatically for the corresponding empty "magnetic" orbitals of minority spin.

As a consequence, the use of Δ^* is required for the azido dimer (less electronegative bridging unit), both Δ and Δ^* can be used for the hydroxo dimer, whereas only Δ is meaningful for the (more electronegative) oxo-bridged dimer, as can be seen in Figs. 3 and 4. The three dimers yield around the same slopes ($K^*_{azido} \approx 1.1$ eV, $K^*_{hydroxo} \approx 1.4$ eV/$K_{hydroxo} \approx 1.7$ eV, and $K_{oxo} \approx 1.1$ eV).

These K values (standing for U of the MO approach, cf. Sect. 2.1) are much smaller than anticipated ($U \approx 5$ eV according to Hay et al. [11]). To understand the reason behind this puzzling result, let us briefly

Table 5. High-spin/broken-symmetry copper spin populations, quantity ΔP^2(Cu), high-spin/broken-symmetry state energies (eV), computed J_{DFT} values (cm^{-1}, from Eq. 8), SOMO gap Δ (eV: majority spin) and corresponding two LUMO gap Δ* (eV: minority spin) for the azido-bridged Cu(II) dimer as a function of the Cu—NH_3 distance. These results are given as obtained for the Cu—Zn copper basis set (see main text)

d(Cu—NH_3)	1.75 Å	2.00 Å	2.50 Å
P_{HS}(Cu)	0.429	0.441	0.404
P_{BS}(Cu)	0.417	0.401	0.337
ΔP^2(Cu)	0.010	0.033	0.050
E_{HS} (eV)	−106.351	−109.572	−108.773
E_{BS} (eV)	−106.362	−109.637	−108.894
J_{DFT} (cm^{-1})	−177	−1048	−1952
Δ	0.362	0.547	0.609
Δ*	0.200	0.359	0.466

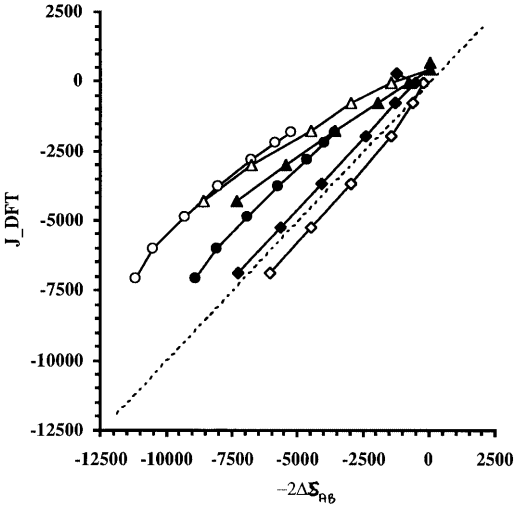

Fig. 2. Plot of J_{DFT} (see Eq. 8) as a function of $-2\Delta S_{AB}$ (*open symbols*) or $-2\Delta^* S_{AB}$ (*filled symbols*) for the azido- (○, ●), hydroxo- (△, ▲), and oxo- (◇, ◆) bridged Cu(II) "core" dimers. The *dashed line* indicates equality between both plotted quantities (cm^{-1})

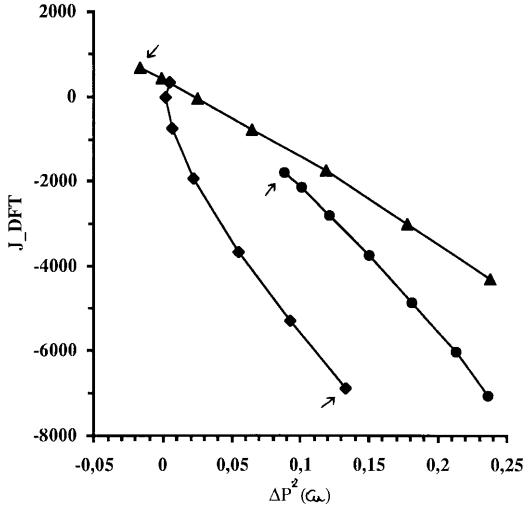

Fig. 1. Plot of J_{DFT} (cm^{-1}: see Eq. 8) as a function of ΔP^2(Cu) for the azido- (●), hydroxo- (▲), and oxo- (◆) bridged Cu(II) "core" dimers. The *arrows* indicate the points computed for the Cu-bridge-Cu angle of 80° (then up to 110°)

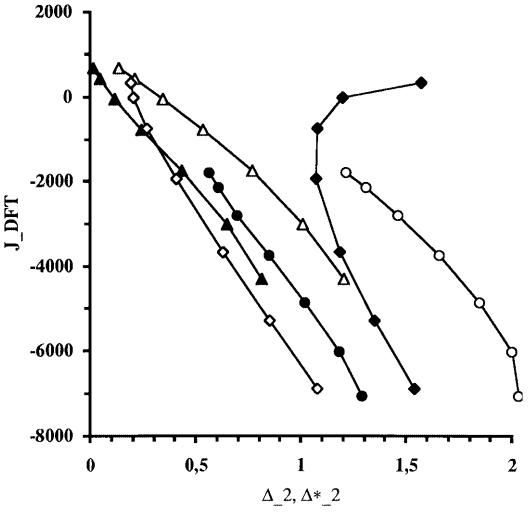

Fig. 3. Plot of J_{DFT} (cm^{-1}: see Eq. 8) as a function of Δ^2 (eV^2: *open symbols*) or $(\Delta^*)^2$ (eV^2: *filled symbols*) for the azido- (○, ●), hydroxo- (△, ▲), and oxo- (◇, ◆) bridged Cu(II) "core" dimers

compare the expression of Hay et al., Kahn and Briat, and Noodleman for the antiferromagnetic contribution to the exchange coupling in the weak overlap regime:

$$\begin{aligned} J_{AF}^{OMO} &\approx -\Delta^2/K \\ J_{AF}^{NMO} &\approx -2\Delta S_{AB} \Rightarrow U \approx 4K \\ J_{AF}^{BS} &\approx -US_{AB}^2 \ . \end{aligned} \tag{9}$$

The derived relation $U \approx 4K$ is about verified, at least for the azido- and oxo-bridged copper dimers. Our results are thus consistent. The reason for the discrepency in the hydroxo case is not obvious.

Notice first that the approximations of Hay et al. ($\Delta \ll K$) may fail because the SOMO gaps (either Δ or Δ^*) are comparable to the K denominator term, in which case their assumption is no longer valid. Moving one step backward in their derivation yields

$$J_{AF} \approx \frac{K}{2} - \sqrt{\Delta^2 + \left(\frac{K}{2}\right)^2} \Rightarrow K \approx \frac{J_{AF}^2 - \Delta^2}{J_{AF}} \ . \tag{10}$$

One thus gets $K^*_{azido} \approx 0.6$ eV, $K^*_{hydroxo} \approx 1.1$ eV/ $K_{hydroxo} \approx 1.7$ eV, and $K_{oxo} \approx 0.8$ eV (values obtained for the largest $|J_{DFT}|$, neglecting there the unknown J_F), values which are even smaller (except for $K_{hydroxo}$) than the previous ones. Notice in passing that, from Eq. (10), $K > 0$ implies $|J_{AF}| < \Delta$, which sets an upper limit to $|J_{AF}|$, as verified from Tables 2–4.

The reason behind this puzzling result (i.e. $U \approx 4K$ instead of $U \approx K$) lies actually in the fact that the BS method overestimates "true" exchange coupling constants, J_{true} by a factor of 2. If one writes in effect $J_{DFT} \approx 2J_{true}$ and equates rather J_{true} with $-\Delta^2/U_{true}$ or $-U_{true}S_{AB}^2$ as should be the case, one derives straightforwardly that $U \approx 2U_{true}$ and $K \approx U_{true}/2$ (where U and K are those derived in Sects. 3.2 and 3.4, respectively), i.e. $U \approx 4K$, as found previously.

4 Discussion and conclusion

We first showed that the VB estimation of J_{DFT} can be expressed only in terms of triplet and BS calculated quantities: $J_{AF} \approx -2\Delta[P_{HS}(Cu)^2 - P_{BS}(Cu)^2]^{1/2}$, whereas quantitative estimates using the alternative MO or VB–BS approaches require knowledge of either K or U (computed directly or obtained from magneto-structural correlations).

Moreover, the quantity $\Delta P^2(Cu)$ appears to be as good an index of the antiferromagnetic contribution to the exchange coupling constant as either Δ^2 or Δ^{*2}. Plotting in effect Δ^2 or Δ^{*2} as a function of $\Delta P^2(Cu)$ yields straight lines for the azido bridge (again for Δ^*), the hydroxo bridge (for both Δ or Δ^*), and the oxo bridge (for Δ), as can be seen in Fig. 5.

Notice also in Table 3 (hydroxo dimer) the occurrence of negative $\Delta P^2(Cu)$ values which do not hinder the generation of a rather linear plot. This also occurs for large angles (130°) in the case of the azido dimer (not shown). This surprising result thus turns J_{AF} into a ferromagnetic term! This peculiar behavior is linked to spin polarization and bridging orbital topology [18]. It can be further rationalized within the VB formalism [19], but this is not the main focus of this article.

Finally, in order to establish the link between the present results, obtained for "bare" copper dimers (i.e. without peripheral ligation) and "real" ones, we selected the azido-bridged species and performed the same analysis as in Sects. 3.2–3.4 for the planar $[Cu_2(N_3)_2(NH_3)_4]^{2+}$ complex, where $d(Cu{-}NH_3)$ was set to 1.75, 2.0 (about the experimental value), and 2.5 Å (Table 5). We could not make this distance greater as the computations no longer converged. This is related to an inherent difficulty of the density functional theory when dealing with the very weak bonding regime [46].

Through their (antibonding) interactions with the peripheral ligand orbitals (favorably located in the magnetic orbital plane), the copper d orbitals rise in

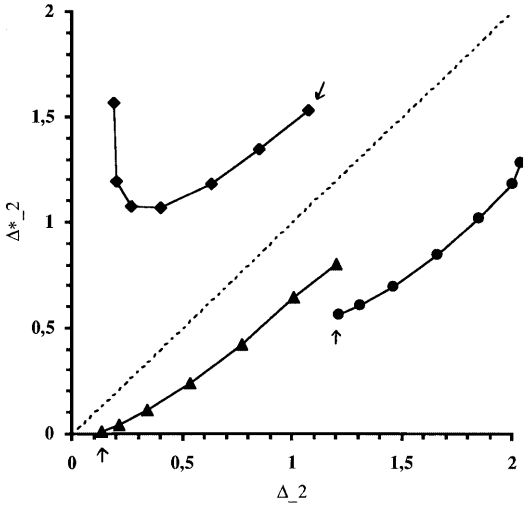

Fig. 4. Plot of $(\Delta^*)^2$ (eV^2) as a function of Δ^2 (eV^2) for the azido- (●), hydroxo- (▲), and oxo- (◆) bridged Cu(II) "core" dimers. The *arrows* indicate the points computed for the Cu-bridge-Cu angle of 80° (then up to 110°)

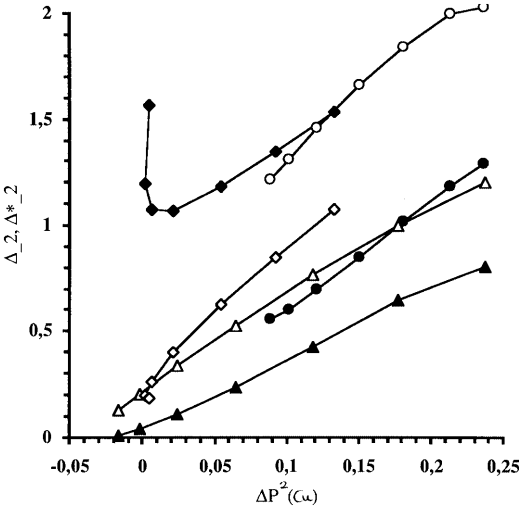

Fig. 5. Plot of Δ^2 (eV^2: *open symbols*) or $(\Delta^*)^2$ (eV^2: *filled symbols*) as a function of ΔP^2(Cu) for the azido- (○, ●), hydroxo- (△, ▲), and oxo- (◇, ◆) bridged Cu(II) "core" dimers

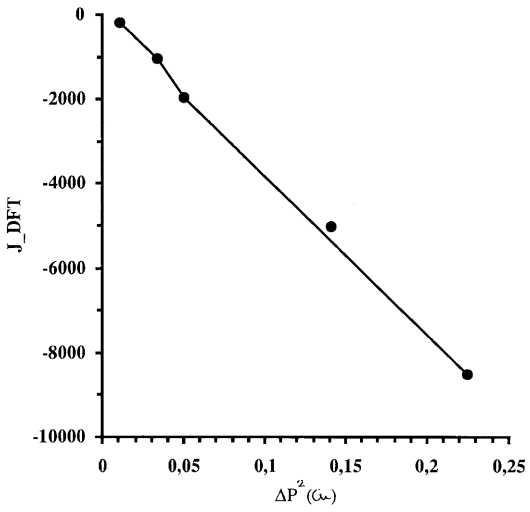

Fig. 6. Plot of J_{DFT} (cm^{-1}: see Eq. 8) as a function of ΔP^2(Cu) for the azido-bridged Cu(II) dimers. The four linked points correspond to the use of the Cu—Zn basis set, the unlinked one to that of Cu—Sd (see main text)

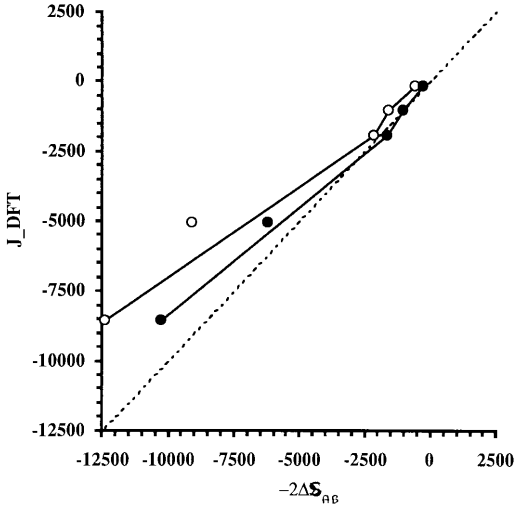

Fig. 7. Plot of J_{DFT} (cm^{-1}: see Eq. 8) as a function of $-2\Delta S_{AB}$ (*open symbols*) or $-2\Delta^* S_{AB}$ (*filled symbols*) for the azido-bridged Cu(II) dimers. The linked points correspond to the use of the Cu—Zn basis set, the unlinked ones to that of Cu—Sd (see main text)

energy, thus diminishing the weight of the bridging ligands (and the magnetic orbital overlap). Both effects combined allow the establishment of ferromagnetism.

We thus plotted J_{DFT} as a function of either ΔP^2(Cu) (Fig. 6), $-2\Delta S_{AB}/-2\Delta^* S_{AB}$ (Fig. 7), or Δ^2/Δ^{*2} (Fig. 8), combining the data from Tables 4 and 5. As can be seen, the use of ΔP^2(Cu) yields a rather satisfying linear plot (with $U \approx 4.8$ eV). The other two plots, illustrating the MO and VB approaches, do not appear to be as reliable when it comes to linking computational results obtained for experimental and infinite Cu—NH_3 distances; however, the use of Δ^* values is still more suitable, a conclusion reached previously.

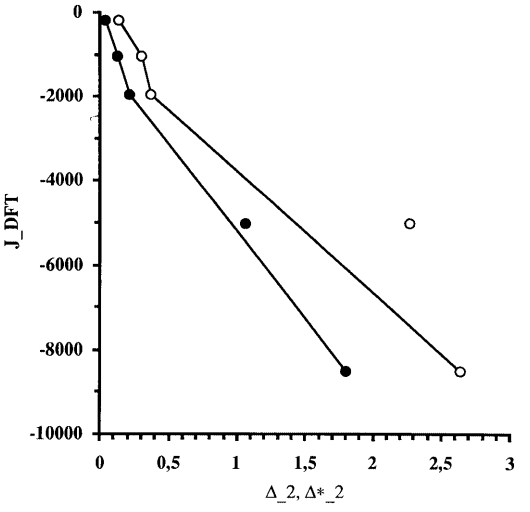

Fig. 8. Plot of J_{DFT} (cm^{-1}: see Eq. 8) as a function of Δ^2 (eV^2: *open symbols*) or $(\Delta^*)^2$ (eV^2: *filled symbols*) for the azido-bridged Cu(II) dimers. The linked points correspond to the use of the Cu—Zn basis set, the unlinked ones to that of Cu—Sd (see main text)

Acknowledgements. We thank the Commissariat à l'Energie Atomique for the use of the CRAY-94 supercomputer in Grenoble.

References

1. Comarmond J, Plumeré P, Lehn J-M, Agnus Y, Louis R, Weiss R, Kahn O, Morgenstern-Badarau I (1982) J Am Chem Soc 104: 6330–6340
2. Sikorav S, Bkouche-Waksman I, Kahn O (1984) Inorg Chem 23: 490–495
3. Mak TCW, Goher MAS (1986) Inorg Chim Acta 115: 17–23
4. von Seggern I, Tuczek F, Bensch W (1995) Inorg Chem 34: 5530–5547
5. Aebersold MA, Gillon B, Plantevin O, Pardi L, Kahn O, Bergerat P, von Seggern I, Tuczek F, Öhrström L, Grand A, Lelièvre-Berna E (1998) J Am Chem Soc 120: 5238–5245
6. Adamo C, Barone V, Bencini A, Totti F, Ciofini I (1999) Inorg Chem 38: 1996–2004
7. Crawford WH, Richardson HW, Wasson JR, Hodgson DJ, Hatfield WE (1976) Inorg Chem 15: 2107
8. Gatteschi D, Kahn O, Miller JS, Palacio F (1991) Magnetic molecular materials. Kluwer, Dordrecht
9. Ruiz E, Alvarez S, Alemany P (1998) Chem Commun 2767–2768
10. Anderson PW (1959) Phys Rev 115: 2–13
11. Hay PJ, Thibeault JC, Hoffmann R (1975) J Am Chem Soc 97: 4884–4899
12. Kahn O, Charlot MF (1980) Nouv J Chim 4: 567–576
13. Girerd JJ, Journaux Y, Kahn O (1981) Chem Phys Lett 82: 534–538
14. Kahn O (1985) In: Willett RD, Gatteschi D, Kahn O (Eds) Magneto-structural correlations in exchange coupled systems. Nato Advanced Study Institute Series C, Vol 140. Reidel, Dordrecht, pp 37–85
15. Charlot M-F, Kahn O, Chaillet M, Larrieu C (1986) J Am Chem Soc 108: 2574–2581
16. Tandon SS, Thompson LK, Manuel ME, Bridson JN (1994) Inorg Chem 33: 5555–5570
17. Thompson LK, Tandon SS, Manuel ME (1995) Inorg Chem 34: 2356–2366
18. Blanchet-Boiteux C, Mouesca J-M (2000) J Am Chem Soc 122: 861–869

19. Blanchet-Boiteux C, Mouesca JM (2000) J Phys Chem A 104: 2091–2097
20. Ruiz E, Alemany P, Alvarez S, Cano J (1997) J Am Chem Soc 119: 1297–1303
21. Ruiz E, Alemany P, Alvarez S, Cano J (1997) Inorg Chem 36: 3683–3688
22. Ruiz E, Cano J, Alvarez S, Alemany P (1998) J Am Chem Soc 120: 11122
23. Daudey J-P, deLoth P, Malrieu J-P (1985) Magneto-structural correlations in exchange coupled systems. NATO Advanced Study Institute Series C, Vol. 140. Reidel, Dordrecht, p 87
24. Astheimer H, Haase W (1986) J Chem Phys 85: 1427
25. Kahn O, Briat B (1976) J Chem Soc Trans II 72: 268
26. Kahn O, Briat B (1976) J Chem Soc Trans II 72: 1441
27. Dunlap BI (1984) Phys Rev A 29: 2902
28. Noodleman L, Case DA (1992) Adv Inorg Chem 38: 423–470
29. Noodleman L (1981) J Chem Phys 74: 5737–5743
30. Hart JR, Rappé AK, Gorun SM, Upton TH (1992) J Phys Chem 96: 6255–6263
31. Hart JR, Rappé AK, Gorun SM, Upton TH (1992) J Phys Chem 96: 6264–6269
32. Caballol R, Castell O, Illas F, Moreira PR, Malrieu JP (1997) J Phys Chem A 101: 7860
33. Ruiz E, Cano J, Alvarez S, Alemany P (1999) J Comput Chem 20: 1391–1400
34. Baerends EJ, Ellis DE, Ros P (1973) Chem Phys 2: 41–51
35. Baerends EJ, Ros P (1973) Chem Phys 2: 52–59
36. Baerends EJ, Ros P (1978) Int J Quantum Chem Quantum Chem Symp 12: 169–190
37. Bickelhaupt FM, Baerends EJ, Ravenek W (1990) Inorg Chem 29: 350–354
38. teVelde G, Baerends EJ (1992) J Comput Phys 99: 84–98
39. Ziegler T (1991) Chem Rev 91: 651–667
40. Vosko SH, Wilk L, Nusair M (1980) Can J Phys 58: 1200
41. Painter GS (1981) Phys Rev B 24: 4264–4270
42. Becke AD (1988) Phys Rev A 38: 3098–3100
43. Perdew JP (1986) Phys Rev B 33: 8822–8824
44. Didziulis SV, Cohen SL, Gewirth AA, Solomon EI (1988) J Am Chem Soc 110: 250
45. Brown CA, Remar GJ, Musselman RL, Solomon EI (1995) Inorg Chem 34: 688
46. Bally T, Narahari-Sastry G (1997) J Phys Chem A 101: 7923–7925